مجلة

كلية التـــراث الجامعة

مجلة علمية محكمة

متعددة التخصصات نصف سنوية

العدد التاسع والثلاثون

عدد خاص بوقائع المؤتمر العلمي السنوي السادس عشر (الدولي الخامس)

18 نيسان 2024

ISSN 2074-5621

رقم الايداع في دار الكتب والوثائق 719 لسنة 2011

مجلة كلية التراث الجامعة معترف بها من قبل وزارة التعليم العالي والبحث العلمي بكتابها المرقم (ب 3059/4) والمؤرخ في (2014/ 4/7)

Studying the Industrial Effect of Copper Oxide Nanoparticles on Carbon Steel in Strong Acid

Sarah Habeeb Jasim* **Taghried Ali Salman****

* Al-Turath University/Al-Nahrain University / Clinical Biochemistry Chemistry Sciences

** Al-Nahrain University/ Department of Chemistry /Physical Sciences

Abstract

In the present study, copper sulphate pentahydrate (CuSO4.5H2O) has been utilized as the (Cu) source and coffee powder extract to create copper oxide nanoparticles (CuONPs) using the sol-gel method at room temperature. CuO NPs was Synthesized with a spherical particle shape (SEM) were examined using (FT-IR) spectroscopy, x-ray diffraction (XRD), ultraviolet-visible spectroscopy (UV-Vis), transmission electron microscopy (TEM), and scanning electron microscopy. The UV-Vis absorption spectrum exhibits an absorption band at 281 nm. By using XRD, it was determined that the finished product was highly crystalline CuO with diameters ranging from 15 to 30 nm. A network of CuO NPs with an average size of 20 nm and a thickness of roughly 8 nm can be seen in the SEM pictures. Studies on weight loss and polarization curves were used to examine the corrosion-inhibiting capability of carbon steel in molar hydrochloric acid solutions. The results showed that as CuONP concentration increased, the effectiveness of prevention also increased. Depending on the isotherm models, the anti-corrosion adsorption process on the surface of carbon steel exhibits Langmuir's behavior as opposed to Freundlich's. According to thermodynamic characteristics, the adsorption mechanism has already been determined to involve exothermic, mixed, and spontaneous adsorption. CuONPs appear to be good carbon steel corrosion inhibitors in acidic settings, and per the research. CuONPs developed a good protective coating on the steel surface of, according to scanning electron microscopy (SEM) photographs.

1.Introduction

Steel alloys are a common engineering material used in many sectors, including construction, transportation, industry, medical, and defense. Corrosion of carbon steel can happen on its own as a result of an electrochemical or chemical reaction with the environment. Hydrochloric acid is necessary for numerous chemical and electrochemical processes, refineries, the metallurgical industry, cleaning specific equipment, and pickling metals. Equipment and devices may corrode severely at high acid concentrations(1).(2) If precautions are not taken, it will affect the environment, social safety, and the strength of the material(3) Uniform, galvanic, pitting, crevice, stress cracking, erosion, and microbiological corrosion are all types of corrosion that can affect carbon steel One of the many proven methods for preventing or decreasing corrosion is to increase the corrosion resistance of carbon steel by adding the proper inhibitors where the corrosion occurs. Corrosion inhibitors are organic compounds with active atoms like S, O, and N that interact with the metallic surface to generate a shielding layer that either stops or slows

corrosion. These chemical substances are pricy, risky, and harmful to the environment (4) The use of environmentally friendly inhibitors has been the subject of numerous scientific research in the past. The bulk of natural products are inexpensive, non-toxic, and biodegradable. Bridelia ferruginea extract is one example of a plant extract.(5) extract from Egyptian brandy seed oil (6) Gmelina arborea bark extracts(7) a loquat leaf(8) and extract from gooseberry husk (9) One of the most exciting academic buildings in nanomaterials nowadays is nanotechnology. Recent studies have concentrated on the design and advancement of plant extract-based nanoparticle biology. Nanotechnology is currently one of the most intriguing research subjects in the field of materials science. They typically consist of compounds that have atoms with high electron densities. Current research focuses on the development and application of nanoparticle biology using a variety of natural extracts. which also have the capacity to produce mineral nanoparticles on the surface of steel, creating a bigger surface area for contact(4,10) Due to their wide range of applications, including superconductors, copper oxide nanostructures have attracted a lot of attention.(11) sensors(12,13) catalytic(14) materials with tremendous magnet resistance(15) sensors for gas(16,17), electricity(18), and optics(19) CuO is a semiconductor with a band gap of 1.7 eV.(20) Transformation of solar energy and creation of composites with organic and inorganic nanostructures It can also be utilized as an antimicrobial, anti-biotic, and anti-fungal agent when added into coatings, plastics, textiles, and other materials(21). The sol-gel technique is one way to produce CuONPs.(22) solid-state reaction method(23) microwave irradiations(24) electrochemical methods(25) the accelerated breakdown of a precursor(26) Some harmful substances that are absorbed on the surface as a result of chemical production procedures may have negative effects in medical applications. Recently, plants like neem have been used to greenly synthesize various nanoparticles.(27) lemon grass(28) Emblica officinalis(29) tamarind (30).

Coffee powder extract was used to create copper oxide nanoparticles (CuONPs), which were then studied using a variety of methods (FTIR, XRD, UV-Vis, TEM, and SEM). Using weight reduction and potentiostatic polarization tests, the effectiveness of CuONPs as a corrosion inhibitor in carbon metal submerged in molar hydrochloric acid solution was demonstrated.

Experiment

1.1. Materials

Each synthetic chemical used in this experiment was of a reasonable quality. Sigma-Aldrich (Darmstadt, Germany) provided 98% of the reagent grade for the ACS reagent (CuSO4.5H2O), 37% HCl.

1.2. Preparation of Coffee Powder Aqueous Extract, the coffee powder was available in a local store in Baghdad, Iraq. To create coffee aqueous extract, 2.5 g of fine coffee powder and 1×102 ml of distilled water were combined in a 300 ml glass beaker. The mixture was heated for 15 minutes at 40 degrees Celsius. The suspension was shaken for 10 minutes at 6,000 rpm after cooling to room temperature, and it was then filtered. The aqueous extract was maintained at 5°C to be used in further research.

1.3. Preparation of cuONPs

In an ideal reaction, 15 mL of distilled water were used to dissolve 2.5 g of copper sulphate pentahydrate (CuSO4.5H2O) in a 250 mL conical flask. five minutes of ambient temperature magnetic swirling in a standard reaction mixture for minutes. the next step is Coffee aqueous extract (30 mL) was added to the The resulting mixture was a copper ion solution.reacted for

six hours at 70 °C in a sand bath with constantly moving. After that, the mixture was cured for four hours at 40 °C, producing the indicated black powder Figure (1) displays the production of copper oxide nanoparticles

1.4**. Hydrochloric acid Solution Preparation**

By diluting 37% HCl with distilled water, a one-molar hydrochloric corrosive arrangement was obtained. The CuONPs were then dissolved in a 100 mL solution of molar hydrochloric acid and stored as a stock solution. The pH of the prepared solution was 2.1. All corrosion investigations employed this 1 M HCl solution in varying concentrations (10–120 ppm), both with and without the inhibitor present.

1.5**. Steel Alloy Preparation**

The carbon steel alloy sample has the following composition, in weight percentages, according to emission spectroscopic analysis: nickel 0.017, phosphor 0.018, carbon 0.19, silicon 0.35, chrome 0.04, copper 0.02, aluminum 0.06, and the remaining iron. Steel samples were reduced in size and shaped into circles, each measuring 1 cm2. 320, 500, 1000, 2400, and 4000 grade emery sheets were used to clean them after that. It was cleaned with acetone, after which it was rinsed with twice-refined water and dried. The resulting mixture was a copper ion solution.

1.6**. CuONPs' Characteristics**

Fourier transform infrared (FTIR) spectroscopic measurements were made using a Shimadzu IR-Prestige-21 spectrophotometer. Using a Schimadzu 1601 spectrophotometer with a resolution of 1 nm and 0.1 ml of the sample combined with 2 ml of deionized water, the ultra violet spectrum of zinc oxide nanoparticles was evaluated as a function of reaction time. The generated copper oxide nanoparticles were examined using a Hitachi S-4500 scanning electron microscope (SEM). Using a Shimadzu XRD-6000 X-ray diffractometer with CuK radiation = 1.5405 throughout a broad range of Bragg angles (30 - 800), powder X-ray diffraction (XRD) was conducted.

1.7. **Surface Characterization**

The morphology of the carbon steel surface was examined for three hours at room temperature with and without 60 ppm of cuONPs using a Hitachi S-4500 SEM type scanning electron microscope.

1.8. **Method of Weight Loss**

Carbon steel alloy was completely dumped in 75 mL of molar hydrochloric acid solution both with and without 10, 30, 60, 90, and 120 ppm inhibitor for three hours at 298 K. After that, the samples were dried, cleaned, and weighed.The corrosion rate (Crate), surface coverage (θ), and efficacy of protection (%I) against weight deficit were measured using the following relations.

$$C_{rate} = \frac{wl}{At} \quad (1)$$

$$\theta = \frac{(W_0 - W_1)}{W_0} \quad (2)$$

$$I\ (\%) = \frac{(W_0 - W_1)}{W_0} \times 100 \quad (3)$$

where A (cm2) denotes the specimen area, t (hr) denotes the immersion period, and W0 and W1 denote the carbon steel weight loss (mg) with and without inhibitor. WL stood for carbon steel weight loss.

1.9. **Research on Potentiostatic**

Electrochemical estimations were made in M Lab using potentiostatic polarization simulations in an electrochemical cell with three cathodes: a platinum counter, a saturated calomel (SCE) as a form of reference, and a carbon steel working electrode. After achieving a consistent state, the working samples were immersed for 15 minutes at 298 K in a test setup of 1 M HCl with and without 10, 30, 60, 90, and 120 ppm inhibitor. The open circuit potential was then measured every fifteen minutes. To ascertain its corrosion proclivity, potentiodynamic polarization simulations were carried out at an output rate of 0.1 mV s-1 throughout a range of 250 mV. Using the information that follows, the inhibitory protection (I %) was determined.

$$I\ \% = \frac{i^{0}_{corr} - i^{1}_{corr}}{i^{0}_{corr}} \times 100 \qquad (4)$$

where the slopes of the Tafel (cathodic and anodic) intercepts are used to estimate the current corrosion densities with and without the inhibitor, respectively, and i_corr^0 and i_corr^1

1. Results and Discussion

1.1. Characterization of CuONPs

Based on electron transfers from the valence band to the conduction. Figure (1. 1)demonstrates a typical excitation absorption at 280 nm, which can be attributed to cuO intrinsic band gap absorption caused by electron transfers from the valence band to the conduction band (O2p-cu 3d). Stretching absorption bands of hydroxyl (-OH) stretching H bonded alcohols and phenols can be attributed to strong at 3,422 and widely scattered absorption bands in the CuONPs FTIR spectra at 1,071 cm-1, respectively (figure 1.2) The TEM pictures of standard and synthetic NPs revealed that the particles are almost spherical in shape, with only minor differences in thickness. Using a histogram, the average particle size was determined to be (25-45, 70.1-90.2) nm, as shown in figure (1.3)and (1.4).

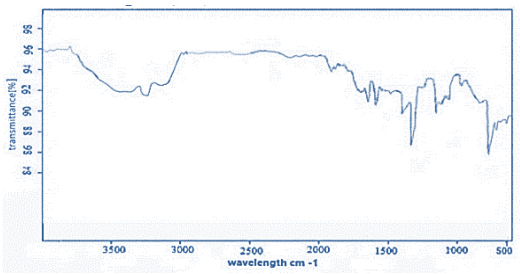

fig (1.2)

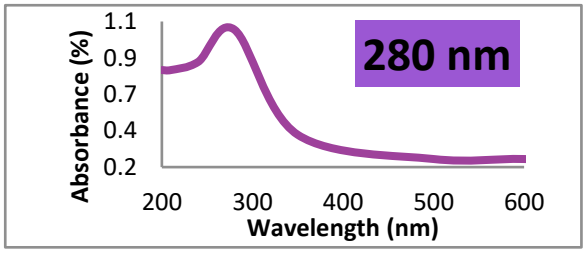

fig (1.1)

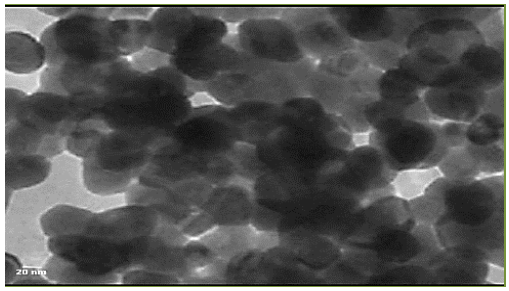

Figure (1.3): TEM image of standard CuO-NPs.

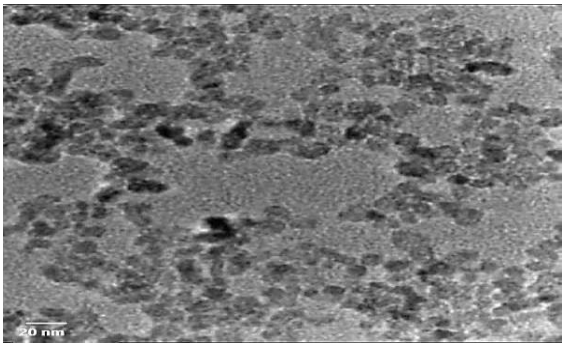

Figure (1.4): TEM image of synthesized CuO-NPs from coffee powder extract.

Most standard and created CuO nanoparticles had well-defined morphologies,spherical in shape with diameters ranging from 20 to 50% nm, and prepared CuO nanoparticles from (55.7-120) 5% nm.

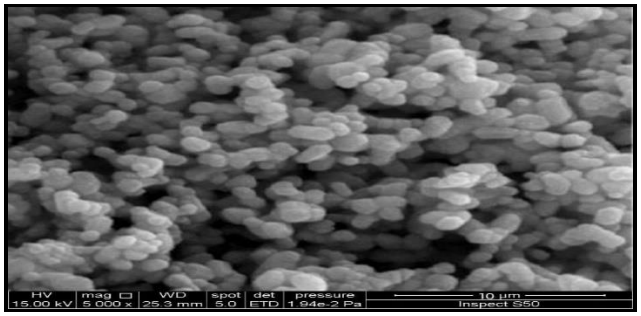

Figure (1.5): SEM images of standrd CuO-NPs.

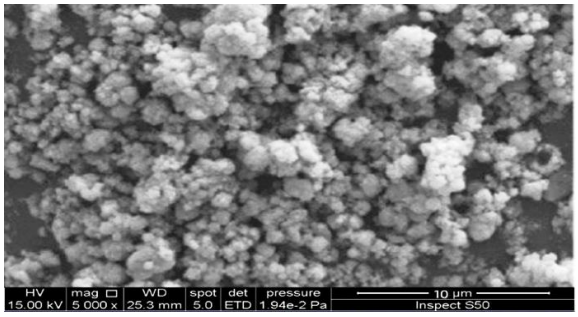

Figure (1.6): SEM images of synthesized CuO-NPs from coffee powder extract.

Figure (1.7) depicts the EDX spectrum analysis analog for produced CuO NPs from coffee powder extract.

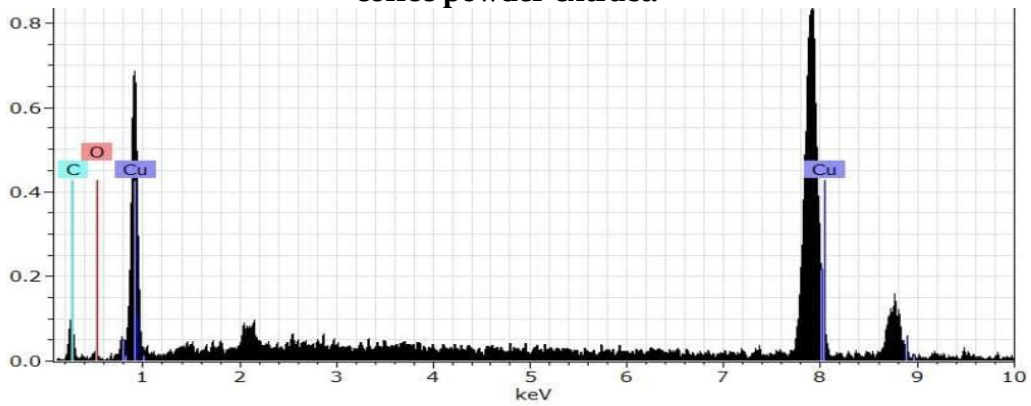

Figure (1.7) the EDX spectrum analysis CuO NPs from coffee powder extract.

From these figures and tables, we can see the peaks of copper and oxygen, which may be associated with a faucal matter that occasionally acts as a capping agent for nanoparticles. When we look at the table, we can see that copper is the most common element, accounting for more than half of the total constituents coupled with oxygen, confirming the creation of pure

copper oxide nanoparticles. This suggests that nanoparticles can be easily synthesized using the biogenic synthesis approach.

1.2. **Weight Loss Method**

In the presence and absence of various CuONPs concentrations, drop in weight measures were used to evaluate the inhibitor's function. A molar hydrochloric acid solution was used to submerge carbon steel electrodes for up to 3 hours. Figure 2 demonstrates that as the inhibitor concentration rises, so do the inhibition efficiency and degree of surface coverage, eventually reaching 60 ppm. Table 1 demonstrates that inhibitor molecules deposited on the carbon steel surface's active sites limit anodic and cathodic processes, enabling CuONPs to be absorbed on the substrate and producing a thin barrier to prevent further corrosion [4,5].

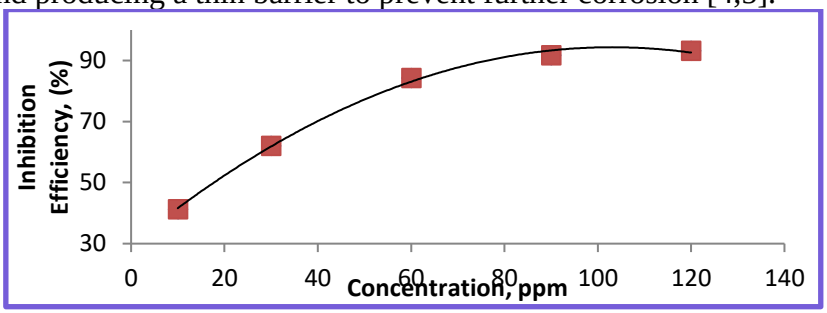

Figure 2. Effect of CuONPs concentrations on the (a) inhibition efficiency (I %) and (b) corrosion rate of carbon steel in 1 MHCl at 298 K.

Table (1): The values of corrosion rate (Crate), Surface coverage (θ) and Inhibition efficiency (I %) for different CuONPs concentrations at 298 K in 1 MHCl solution**.**

C/ (ppm)	C_{rate} ($mg.cm^{-2}.hr.^{-1}$)	θ	I (%)
Blank	1.20	-	-
10	0.38	0.41	41.25
30	0.17	0.62	62.02
60	0.09	0.88	84.22
90	0.06	0.91	91.74
120	0.02	0.93	93.18

Potensiostatic Polarization Studies 3.3

Figure3 depicts the potentiostatic polarization plots Tafel lines (both anodic and cathodic) for steel corrosion in molar hydrochloric acid solution with and without different concentrations of CuONPs at 298 K. The Tafel slopes reveal that adding an inhibitor affects both anodic and cathodic processes, indicating that CuONPs inhibitors have a mixed effect. When CuONPs concentrations approach 60 ppm or higher, the carbon steel surface becomes saturated with inhibitor molecules, causing the Tafel anodic and cathodic curves, as well as inhibitory efficacy values, to shift [21].

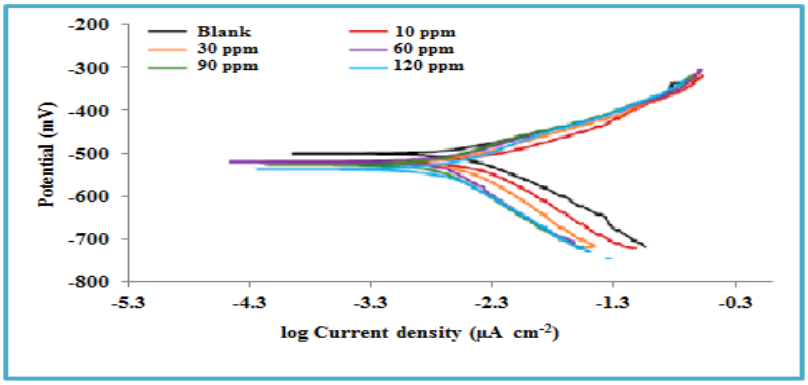

Figure 3. Polarization behavior of carbon steel corrosion in acid 1 M HCl in the presence of different concentrations of cuONPs at 298 K.

Table (3-11): The values of corrosion rate (Crate), Surface coverage (θ) and Inhibition efficiency (I %) for different CuONPs concentrations at 298 K in 1 MHCl solution**.**

C/ (ppm)	C_{rate} (mg.cm^{-2}.hr.$^{-1}$)	θ	I (%)
Blank	1.20	-	-
10	0.38	0.41	41.25
30	0.17	0.62	62.02
60	0.09	0.88	84.22
90	0.06	0.91	91.74
120	0.02	0.93	93.18

It is significant to note that the rate of corrosion decreased as the inhibitor concentration increased. This means that at a concentration of 120 ppm at 298 K, the inhibitor is 93% effective, as indicated in Table 1. In addition to the molecules in the coffee powder extract, the presence of CuONPs on the steel surface creates a barrier that protects anodic and cathodic processes, slowing corrosion [20].

3.4 Models of Thermodynamic Adsorption

The Langmuir and Freundlich models were used to characterize the interactions between the adsorbent copper oxide nanoparticles and the carbon steel surface. The degree of surface covering was determined using potentiostatic data. Using the adsorption isotherm modeling models [17.18]:

Langmuir equation: - $\frac{C_{inh}}{\theta} = \frac{1}{K_{ads}} + C_{inh}$ (5)

Freundlich equation: - $\ln \theta = \ln K_{ads} + \frac{1}{n} \ln C_{inh}$ (6)

where Kads is the ideal adhesion factor, and n measures the adsorption intensity. The adsorption isotherm graphs are shown in Figure 5.

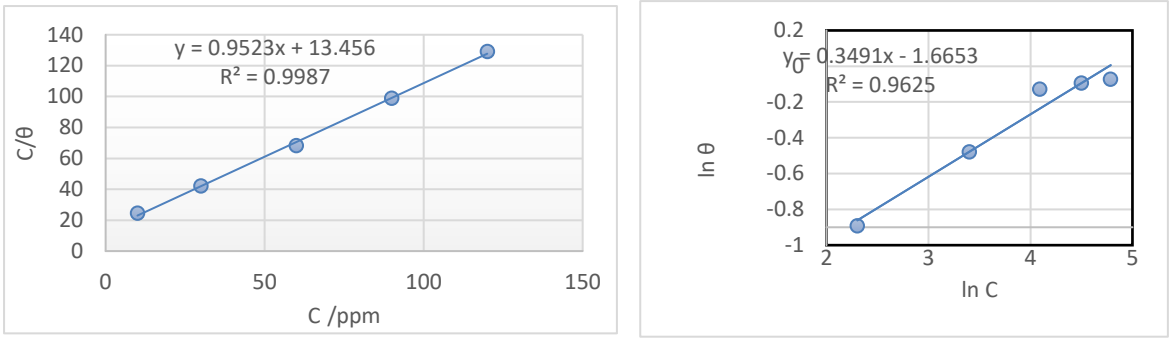

Figure (5) shows the Langmuir and Freundlich isotherms for the adsorption of CuONP molecules on the surface of carbon steel.

When compared to Freundlich, where the correlation coefficient (R2) was nearly unity, the Langmuir isotherm model provided the best fit. Using equation [7], the standard Gibbs free energy (ΔGads) was calculated from the thermodynamic constant of adsorption (Kads) using the following relation:

$$\Delta G^{o}_{ads} = -RT \ln (55.5\, K_{ads}) \quad (7)$$

R is the universal gas constant, T is absolute temperature, and 55.5 is water's adsorption molar heat. The adsorption Gibbs free energy (ΔG◦ads) values were -30.744 kJ/mol for zinc and copper oxide nanoparticles, respectively. The data collected show that the adsorption of both nanoparticles on carbon steel surfaces is spontaneous. The ΔG◦ads value reveals that the adsorption is chemical and supports the experimental findings.

3.4. Scanning Electron Microscopy (SEM)

The carbon steel surface was examined using a SEM instrument after being immersed in 1 M HCl solution for 3 hours in the absence and presence of 120 ppm CuONPs. Figure 6 shows that the carbon steel in the blank solution was significantly corroded, with fissures and holes on its surface, as well as scratching; however, corrosion was avoided in the presence of an inhibitor, and the surface was free of pits and cracks, with only a few scratches [1,3,4]. CuONP layers were discovered on the steel surface, resulting in the formation of an outer coating. As a result, CuONPs are recommended for use as a corrosion inhibitor in HCl-treated carbon steel.

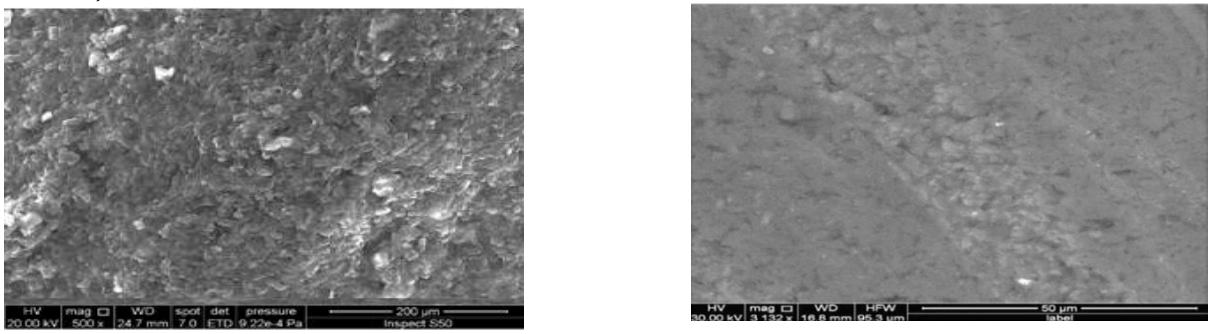

Figure (6) shows a SEM picture of carbon steel (A) polished alloy (B) immersed in 1 M HCl, and (C) in the presence of 120 ppm CuONPs for 3 hours at 298 K.

3.6. Corrosion Inhibition Mechanism

As demonstrated in the equations below, the CuONPs and coffee extract contained in HCl are transported to the surface of the carbon steel, where iron and hydrogen ions are seen on the anodic and cathodic active sites, respectively

$Fe \rightarrow Fe^{2+} + 2e^{-}$ (anodic reaction)

$2H^{+} + 2e^{-} \rightarrow H_{2(g)}$ (cathodic reaction)

When a hydrochloric acid solution is exposed to the environment, the dissolved oxygen is transformed to water: O2 + 4H+ + 4e- → 2H2O (oxygen reduction reaction).

Coffee extract active groups and ferric ions combined with copper oxide nanoparticles to form a complex at the interface of carbon steel and hydrochloric acid solution, Fe2+, CuONPs-coffee extract. Because this chemical occupies active anodic sites, the corrosion rate is slowed [1,3]. The adsorption mechanism of inhibitor molecules on the surface of carbon steel is described as follows: the inhibitor molecules are adsorbed on the surface of the carbon steel via electrostatic interaction between electrons deposited on the surface of the carbon steel (physical adsorption). Chemical adsorption is facilitated by the presence of heteroatoms with a free electron pair.Carbon steel's surface gets more negative as electrons accumulate on it. This enables electron transfer from the Fe orbitals to the inhibitor molecules' non-bonding orbitals, resulting in improved inhibitor adsorption on the carbon steel surface. [4,10].

3.7. **Conclusion**

Coffee extract can be utilized to produce CuONPs. According to the results of weight loss and active polarization experiments, CuONPs is a potent carbon steel corrosion inhibitor in 1 M HCl. The efficiency of inhibition increases with increasing CuONP concentrations. It has a 93% inhibitory efficacy, indicating that it can also function as a mixed-type inhibitor. The carbon steel corrosion inhibition mechanism closely resembled the Langmuir isotherm (R2 = 0.998) rather than the Freundlich isotherm (R2 = 0.9625). According to the calculated Gads value, the adsorption of the inhibitor molecules on the metal surface was spontaneous, and the adsorption of the inhibitor molecules on the metal surface was the result of the chemical adsorption mechanism through heteroatoms with a free electron pair, as well as the decomposition mechanism by electrostatic interaction between the electrons adsorbed on the surface of carbon steel.

Depending on the SEM study data, cuONPs can operate as a carbon steel corrosion inhibitor in 1 M hydrochloric acid solutions, where the formation of a complex of ferric (Fe+2) and copper oxide nanoparticles (cuONPs) coffee extract on the carbon steel/HCl solution interface slows the corrosion rate.

References.

1. Zhao CY, Lu TJ, Hodson HP, Jackson JD. The temperature dependence of effective thermal conductivity of open-celled steel alloy foams. Materials Science and Engineering: A. 2004 Feb 25;367(1–2):123–31.
2. Tariq Saeed M, Saleem M, Usmani S, Malik A, Al-Shammari A, Deen M. Corrosion inhibition of mild steel in 1 M HCl by sweet melon peel extract. 2019 [cited 2023 Oct 11]; Available from: https://doi.org/10.1016/j.jksus.2019.01.013
3. Mainieri T, Barnett EG, Valdero TR, Unipan JB, Oskamp S. Green Buying: The Influence of Environmental Concern on Consumer Behavior. J Soc Psychol [Internet]. 1997 Apr 1 [cited 2023 Oct 11];137(2):189–204. Available from: https://www.tandfonline.com/doi/abs/10.1080/00224549709595430

4. Salman TA, Sabri M, Taghried C, Salman A. Pomegranate Peel Extract as Green Corrosion Inhibitor for α-Brass in 2M HCl Solution. 2017 [cited 2023 Oct 12]; Available from: http://www.jmsse.org/&http://www.jmsse.in/
5. Said-Al Ahl H, Hussein MS, Gendy ASH, Tkachenko KG. Quality of Sage (Salvia officinalis L.) Essential Oil Grown in Egypt. International Journal of Plant Research [Internet]. 2015 [cited 2023 Oct 12];1(4):119–23. Available from: http://www.aiscience.org/journal/ijprhttp://creativecommons.org/licenses/by-nc/4.0/
6. Iroha NB, Akaranta O. Experimental and surface morphological study of corrosion inhibition of N80 carbon steel in HCl stimulated acidizing solution using gum exudate from Terminalia Mentaly. SN Appl Sci [Internet]. 2020 Sep 1 [cited 2023 Oct 12];2(9):1–11. Available from: https://link.springer.com/article/10.1007/s42452-020-03296-8
7. Zheng X, Gong M, Li Q, Guo L. Corrosion inhibition of mild steel in sulfuric acid solution by loquat (Eriobotrya japonica Lindl.) leaves extract. Scientific Reports 2018 8:1 [Internet]. 2018 Jun 14 [cited 2023 Oct 12];8(1):1–15. Available from: https://www.nature.com/articles/s41598-018-27257-9
8. Dehghani A, Bahlakeh G, Ramezanzadeh B, Ramezanzadeh M. Potential of Borage flower aqueous extract as an environmentally sustainable corrosion inhibitor for acid corrosion of mild steel: Electrochemical and theoretical studies. J Mol Liq. 2019 Mar 1;277:895–911.
9. Al-Dahiri RH, Turkustani AM, Salam MA. The Application of Zinc Oxide Nanoparticles as An Eco-Friendly Inhibitor for Steel in Acidic Solution. Int J Electrochem Sci. 2020 Jan 1;15(1):442–57.
10. Somoghi R, Purcar V, Alexandrescu E, Gifu IC, Ninciuleanu CM, Cotrut CM, et al. Synthesis of Zinc Oxide Nanomaterials via Sol-Gel Process with Anti-Corrosive Effect for Cu, Al and Zn Metallic Substrates. Coatings 2021, Vol 11, Page 444 [Internet]. 2021 Apr 13 [cited 2023 Oct 12];11(4):444. Available from: https://www.mdpi.com/2079-6412/11/4/444/htm
11. Yip SK, Sauls JA. Nonlinear Meissner effect in CuO superconductors. Phys Rev Lett [Internet]. 1992 Oct 12 [cited 2023 Oct 12];69(15):2264. Available from: https://journals.aps.org/prl/abstract/10.1103/PhysRevLett.69.2264
12. Kim YS, Hwang IS, Kim SJ, Lee CY, Lee JH. CuO nanowire gas sensors for air quality control in automotive cabin. Sens Actuators B Chem. 2008 Dec 10;135(1):298–303.
13. Umar A, Rahman MM, Al-Hajry A, Hahn YB. Enzymatic glucose biosensor based on flower-shaped copper oxide nanostructures composed of thin nanosheets. Electrochem commun. 2009 Feb 1;11(2):278–81.
14. Yang S, Wang C, Chen L, Chen S. Facile dicyandiamide-mediated fabrication of well-defined CuO hollow microspheres and their catalytic application. Mater Chem Phys. 2010 Apr 15;120(2–3):296–301.
15. Acharyulu NPS, Dubey RS, Swaminadham V, Kollu P, Kalyani RL, Pammi SVN. Green Synthesis of CuO Nanoparticles using Phyllanthus Amarus Leaf Extract and their Antibacterial Activity Against Multidrug Resistance Bacteria Green synthesis of CuO nanoparticles. [cited 2023 Oct 12]; Available from: www.ijert.org
16. Ishihara T, Higuchi M, Takagi T, Ito M, Nishiguchi H, Takita Y. Preparation of CuO thin films on porous BaTiO3 by self-assembled multibilayer film formation and application as a CO2 sensor. J Mater Chem [Internet]. 1998 Jan 1 [cited 2023 Oct 13];8(9):2037–42. Available from: https://pubs.rsc.org/en/content/articlehtml/1998/jm/a801595c
17. Ishihara T, Kometani K, Hashida M, Takita Y. Application of Mixed Oxide Capacitor to the Selective Carbon Dioxide Sensor: I . Measurement of Carbon Dioxide Sensing Characteristics. J

Electrochem Soc [Internet]. 1991 Jan 1 [cited 2023 Oct 13];138(1):173–6. Available from: https://iopscience.iop.org/article/10.1149/1.2085530
18. Podhájecký P, Klápště B, Novák P, Mrha J, Moshtev R, Manev V, et al. The influence of preparation conditions on the electrochemical behaviour of CuO in a Li/CuO cell. J Power Sources. 1985 Apr 1;14(4):269–75.
19. Chiong Cheong F, Yu T, Cheong FC, Sow CH. The manipulation and assembly of CuO nanorods with line optical tweezers. Nanotechnology [Internet]. 2004 [cited 2023 Oct 12];15:1732–6. Available from: https://www.researchgate.net/publication/231086218
20. Vijaya Kumari K. ADENOMYOSIS AYURVEDIC INTERVENTION : CASE REPORT.
21. Vijay Kumar R, Elgamiel R, Diamant Y, Gedanken A, Norwig J. Sonochemical Preparation and Characterization of Nanocrystalline Copper Oxide Embedded in Poly(vinyl alcohol) and Its Effect on Crystal Growth of Copper Oxide. Langmuir [Internet]. 2001 Mar 6 [cited 2023 Oct 13];17(5):1406–10. Available from: https://pubs.acs.org/doi/abs/10.1021/la001331s
22. Naika HR, Lingaraju K, Manjunath K, Kumar D, Nagaraju G, Suresh D, et al. Green synthesis of CuO nanoparticles using Gloriosa superba L. extract and their antibacterial activity. Journal of Taibah University for Science [Internet]. 2015 [cited 2023 Oct 13];9(1):7–12. Available from: https://www.tandfonline.com/doi/abs/10.1016/j.jtusci.2014.04.006
23. Xu C, Liu Y, Xu G, Wang G. Preparation and characterization of CuO nanorods by thermal decomposition of CuC2O4 precursor. Mater Res Bull. 2002 Nov 20;37(14):2365–72.
24. Wang H, Xu JZ, Zhu JJ, Chen HY. Preparation of CuO nanoparticles by microwave irradiation. J Cryst Growth. 2002 Sep 1;244(1):88–94.
25. Yin AJ, Li J, Jian W, Bennett AJ, Xu JM. Fabrication of highly ordered metallic nanowire arrays by electrodeposition. Appl Phys Lett [Internet]. 2001 Aug 13 [cited 2023 Oct 13];79(7):1039–41. Available from: /aip/apl/article/79/7/1039/114597/Fabrication-of-highly-ordered-metallic-nanowire
26. Xu C, Liu Y, Xu G, Wang G. Preparation and characterization of CuO nanorods by thermal decomposition of CuC2O4 precursor. Mater Res Bull. 2002 Nov 20;37(14):2365–72.
27. Shankar SS, Rai A, Ahmad A, Sastry M. Rapid synthesis of Au, Ag, and bimetallic Au core–Ag shell nanoparticles using Neem (Azadirachta indica) leaf broth. J Colloid Interface Sci. 2004 Jul 15;275(2):496–502.
28. Shankar SS, Rai A, Ankamwar B, Singh A, Ahmad A, Sastry M. Biological synthesis of triangular gold nanoprisms. Nature Materials 2004 3:7 [Internet]. 2004 Jun 20 [cited 2023 Oct 13];3(7):482–8. Available from: https://www.nature.com/articles/nmat1152
29. Ankamwar B, Damle C, Ahmad A, Sastry M. Biosynthesis of Gold and Silver Nanoparticles Using Emblica Officinalis Fruit Extract, Their Phase Transfer and Transmetallation in an Organic Solution. J Nanosci Nanotechnol. 2005;5(10):1665–71.
30. Ankamwar B, Chaudhary M, Sastry M. Gold Nanotriangles Biologically Synthesized using Tamarind Leaf Extract and Potential Application in Vapor Sensing. Synthesis and Reactivity in Inorganic, Metal-Organic and Nano-Metal Chemistry [Internet]. 2005 [cited 2023 Oct 13];35(1):19–26. Available from: https://www.tandfonline.com/doi/abs/10.1081/SIM-200047527